

Direction-aware optoelectronic fiber gyroscope

MOHAMED SHALABY^{a,*}, IBRAHIM SAYED^b, KHALED SHARAF^b

^a*Al Imam Mohammad Ibn Saud Islamic University, College of Engineering, Electrical Engineering Department, Riyadh, Saudi Arabia*

^b*Ain Shams University, Faculty of Engineering, Electronics and Communications Department, Cairo, Egypt*

We present, for the first time to our knowledge, a new fiber gyroscope scheme based on an optoelectronic oscillator OEO. The OEO is modified by adding another fiber loop in such a way that the new scheme is composed of an all optical "AO" cavity coupled to an optoelectronic "OE" cavity. The new optoelectronic fiber gyroscope OEFG is capable of not only measuring the angular rotation speed but also of determining the direction of rotation which is not possible in existing fiber laser gyroscopes without the inclusion of complicated setup.

(Received January 18, 2019; accepted August 20, 2019)

Keywords: Optoelectronic, Oscillator, Fiber gyroscope

1. Introduction

Gyroscopes are devices designed to measure angular velocity. There are different types of gyroscopes, mechanical, acousto-optic [8], and optical gyroscopes [7, 9].

Optoelectronic gyroscopes are classified under optical gyroscopes. First, the basic principle of laser gyroscope operation is to allow the buildup of laser oscillations in clockwise and counter-clockwise directions in the same laser cavity. These two sets of laser oscillations should be kept uncoupled to ensure having a laser gyroscope capable of sensing rotation. Therefore, the lasing condition results in two sets of uncoupled modes. The modes separation frequency " f_{FSR} " is determined by the cavity loop length "L" through the relation $f_{FSR} = \frac{c}{nL}$ where n is the laser medium refractive index. If the whole system rotates in the counter clockwise direction, the path length in the optical loop in the clockwise direction is shortened, while in the other direction is elongated. The oscillating modes in the clockwise direction shift towards higher frequencies but those in the counter-clockwise direction shift towards lower frequencies. Since these two groups of oscillations mix at the photodetector which produces a beating signal whose frequency is equal to the shift occurring and this frequency is an indication of the angular rotation speed. Changing the direction of the rotation causes those modes which previously shifted to higher frequencies to shift in this case to lower frequencies and vice versa. At the output of the photodetector, the frequency of the detected RF signal indicates again the angular rotation speed but lacks information about the direction of rotation.

In this single cavity laser gyroscope, the phase condition of oscillating modes is given by;

$$\varphi = \frac{n\omega_0}{c}L = 2m\pi \quad (1)$$

where, ω_0 is the optical oscillation frequency, and m is an integer

In case of laser cavity rotation, the phase condition should be maintained and therefore the oscillation frequencies of the laser modes change according to,

$$\Delta\varphi = 0 = \frac{n}{c}(\omega_0\Delta L + L\Delta\omega) \quad (2)$$

From which,

$$\Delta\omega = -\omega_0 \frac{\Delta L}{L} \quad (3)$$

If a laser loop of radius "R" is rotating at an angular velocity " Ω " and the optical wave transit time in the laser loop is " τ " where;

$$\tau = \frac{nL}{c} \quad (4)$$

then we arrive at the shift in modes frequencies " $\Delta\omega$ " as follows,

$$\Delta\omega = -\frac{\omega_0\Omega nL}{2\pi c} \quad (5)$$

2. Analysis

The idea of the new scheme is completely different which is based on strong coupling between the two groups of modes (see Fig. 1).

The new setup consists of two coupled loops [1-6]:

A. All optical loop, which comprises two optical couplers and an optical fiber coil. This passive loop is driven by an external laser diode source.

B. hybrid active loop (optoelectronic) which comprises a laser diode source, two fiber couplers, a fiber coil, a photodetector, an electronic filter, and a phase

shifter. It should be noted that the fiber coil sensing the rotation holds a wave propagating in one direction only.

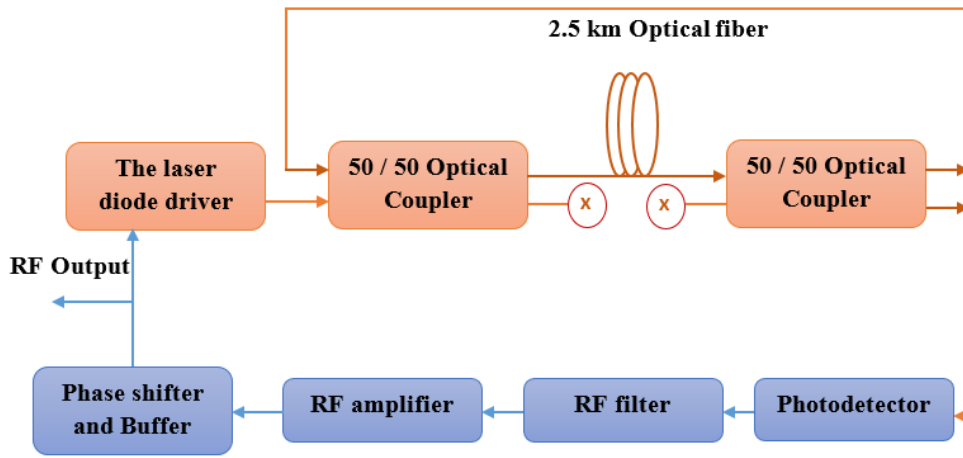


Fig. 1. Schematic diagram of an OEFG

The beating of the optical cavity modes produced by the photodetector results in RF signals at frequencies multiples of the modes separation frequency ($m f_{FSR}$ where $m = 1, 2, 3, \dots$). The electronic filter is adjusted at one of these frequencies ($4f_{FSR}$ in our case). The adjustable phase shifter is added to cancel the phase shift produced by the electronic amplifier and the filter and to adjust the phase of this cavity. The oscillating optical modes are hence separated accordingly by $4f_{FSR}$ and not f_{FSR} due to the filter effect (see Fig. 2). As a result of figure (2) the optical intensity is in this case modulated at $4f_{FSR}$.

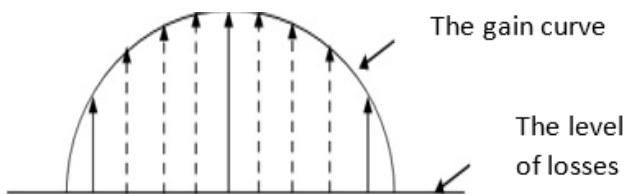


Fig. 2. The modes appearing in dashed lined are not able to oscillate due to the electronic filter adjusted in this simple example at four times the free spectral range frequency

Why this new configuration is able to sense the direction of rotation?

The case of coupled cavity gyroscope we study here is different. The length "L" of the optical loop causes a phase, which should be equal to the phase of the hybrid optoelectronic loop. Rotation of the setup causes the phase seen by the signal in the optical loop to change according to,

$$\Delta\varphi = \frac{n\omega_0}{c} \Delta L \quad (6)$$

$$\Delta\varphi = 2\pi n^2 R L \frac{\Omega}{c\lambda} \quad (7)$$

Hence the operating RF frequency in the hybrid loop should change in such a way to produce a phase shift change counteracting that occurring due to rotation in the optical loop (since the two cavities are coupled). Biasing the electronic system such that the electronic phase relation is linear with RF frequency deviation from the central frequency makes the OEFG capable of sensing the direction of rotation and producing a linear scale factor as we will demonstrate below.

In what follows we will measure the shift in the RF frequency produced by rotation.

3. Setup

The Optoelectronic Fiber Gyroscope Consists of two main parts:

- Electrical part.
- Optical part.

The electronic part

The electronic part contains four main components:

- Band-pass Filter.
- Amplifier.
- Phase shifter.
- Buffer.

The Band pass filter

We used the RF LC tunable filter. This type of filters offers a high quality factor and in our case it can be tuned and adjusted easily in the range 350- 500 kHz

The non-inverting amplifier, the phase shifter, and the buffer are designed using Op-Amp LF 351N. The buffer is added to prevent loading effect of the laser diode driver on the phase shifter.

The optical part

The optical part contains four main components:

- The Laser Diode Driver.
- Delay line
- Optical coupler, and
- Photo Detector.

The Laser Diode Driver

The Laser Diode driver acts as an intensity modulator at $\lambda=1310\text{nm}$.

The Delay Line

The delay line used is an optical fiber with the following parameters:

- Single mode silica fiber.
- 2500 m long.
- $\alpha=0.35\text{ dB/Km}$ at $\lambda=1310\text{ nm}$
- Dispersion: -1.9ps / km.nm

Optical coupler

Two 50/50 optical couplers are used.

The Photo Detector

The Photo detector used is an InGaAs Amplified detector working at $\lambda=700\text{-}1800\text{nm}$. The scale factor of the detector is $0.01\text{ Volt}/\mu\text{W}$.

4. Experimental results

When first setting up the system we use the open loop configuration as shown in Fig. 3, to adjust the input signal (from a signal generator) with the output signal to be in phase and having same amplitude. After adjusting the open loop configuration and getting sure the input and the output are the same in amplitude and phase as shown in Fig. 4, we close the loop to operate in the closed loop configuration and measure the output.

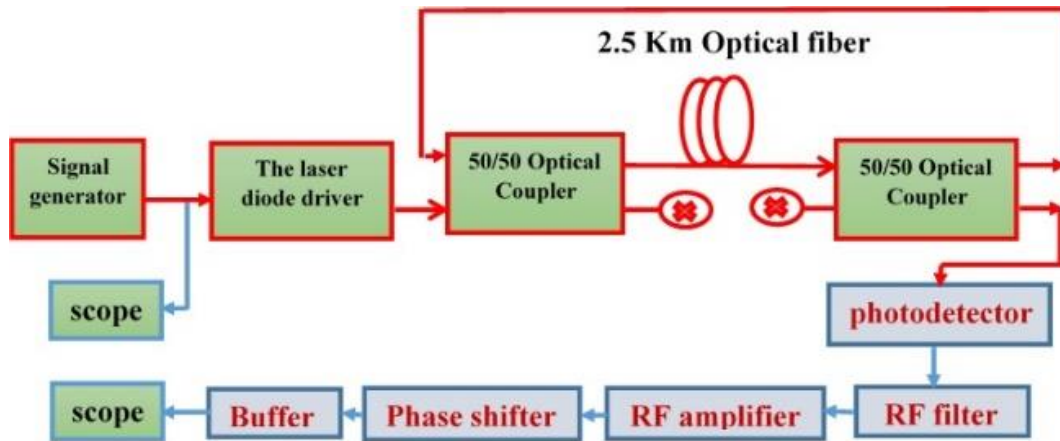


Fig. 3. The open loop configuration of an OEFG

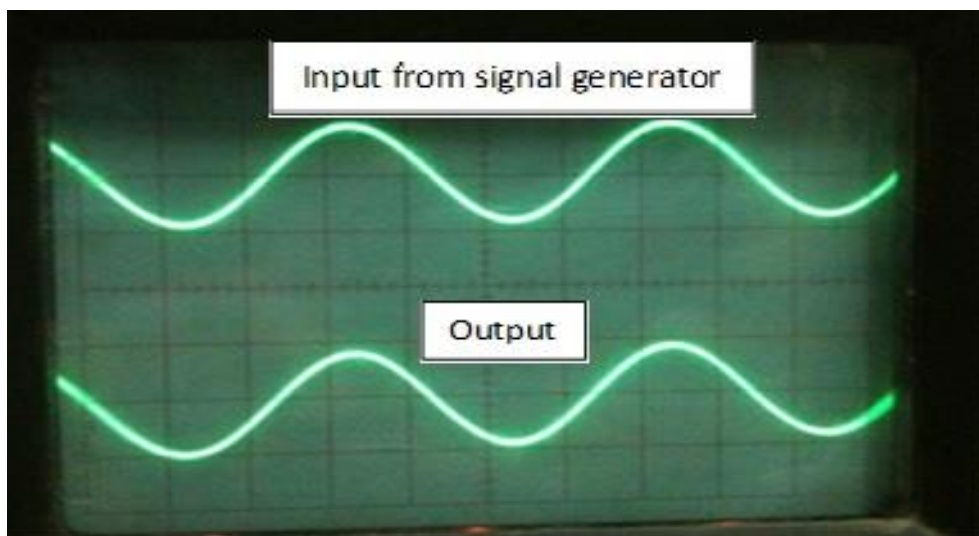


Fig. 4. The output from open loop configuration

Without rotation

If this configuration is stationary (without rotation), the optical loop oscillates in certain modes. The beating of

these modes at the photodetector produces RF signals at frequencies multiples of the modes separation frequency ($m f_{\text{FSR}}$ where $m = 1, 2, 3 \dots$) BPF filter selects one of these beating frequencies which is adjusted in our case at $4f_{\text{FSR}} =$

468.5 kHz as shown on the RF spectrum analyzer (see Fig. 5).

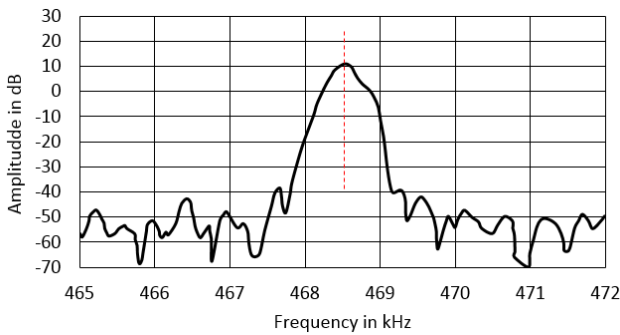


Fig. 5. The RF spectrum of cavity output without rotation

Case of rotation

The output of Optoelectronic Fiber Gyroscope in case of counter clockwise rotation (see Fig. 6), where $\Delta f = 1050 \text{ Hz @ } \Omega = 4.75^\circ/\text{sec}$

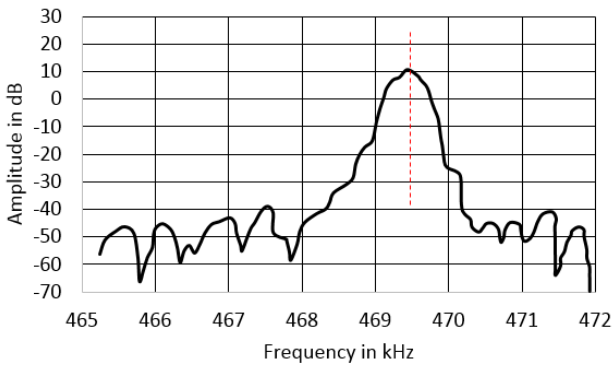


Fig. 6. RF spectrum of cavity output when the setup is rotating counter clockwise @ $\Omega = 4.75^\circ/\text{sec}$

The output of Optoelectronic Fiber Gyroscope in case of clockwise rotation (see Fig. 7), where $\Delta f = -1050 \text{ Hz @ } \Omega = 4.75^\circ/\text{sec}$

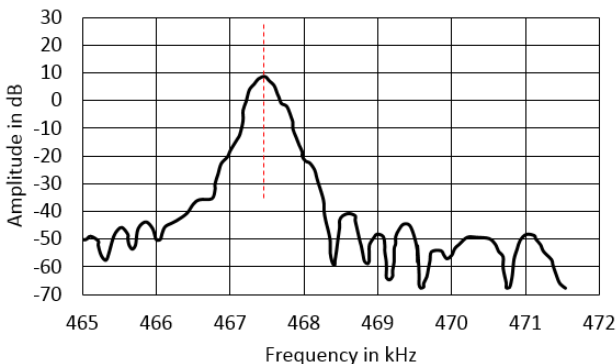


Fig. 7. RF spectrum of cavity output when the setup is rotating clockwise @ $\Omega = 4.75^\circ/\text{sec}$

5. Optoelectronic fiber gyroscope parameters

5.1. Scale factor

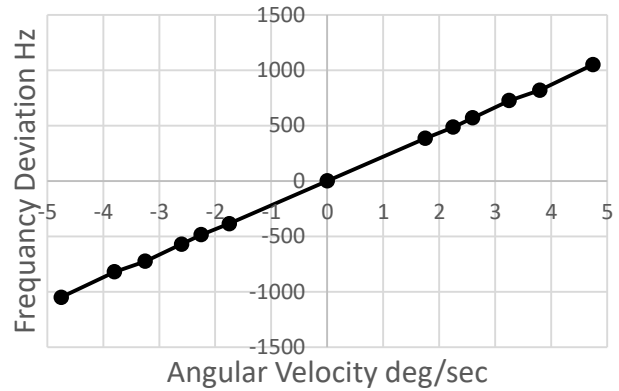


Fig. 8. The frequency deviation curve

As a numerical example for the case of our setup

$R=0.1 \text{ m, } \lambda=1.3 \mu\text{m, and } \Omega=4.75^\circ/\text{sec}$, then the shift in phase is given by $\Delta\phi = 0.722 \text{ rad}$

The scale factor = $1050/4.75=221.1 \text{ Hz}/(\text{deg}/\text{sec})$ (see Fig. 8).

Fig. 9 show the scale factor linearity within the dynamic range between $\pm 5 \text{ deg}/\text{sec}$ which shows a good linearity in this range.

Scale Factor Linearity

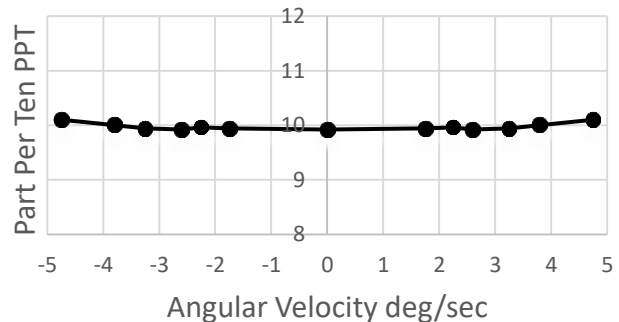


Fig. 9. The Scale factor Linearity curve

5.2. Resolution

According to Fig. 5 the -3 dB bandwidth of the photodetector output is around 250 Hz. This bandwidth is a combined result of the implemented electronic circuits along with that of the optical modes bandwidth. This measured bandwidth corresponds to a rotation rate $\Omega = 1^\circ/\text{sec}$ this can be considered as the minimum detectable rotation rate (system resolution).

Regarding the dynamic range of measured velocities of this gyroscope, it is mainly related to the bandwidth of

the used electronic parts (the amplifier, the phase shifter, and the buffer).

Phase noise and hence angle random walk of this type of gyroscopes is better than fiber laser gyroscopes due to the inclusion of a band pass filter [10, 11].

6. Conclusion

We have demonstrated a new scheme of an optoelectronic fiber laser gyroscope capable of measuring the angular speed and identifying the direction of rotation. The simple analytic study of the system given is in good agreement with the experimental results obtained. To increase the scale factor of the optoelectronic gyroscope we propose building a new setup with a bandpass filter at a higher central frequency.

Acknowledgments

The authors would like to thank the Deanship of Scientific Research at Al Imam Mohammad Ibn Saud Islamic University, Saudi Arabia for financing this project under the grant no. (381404), and for the continuous help during this work by providing the space and equipment required to carry out the experimental measurements.

References

- [1] M. Shalaby, I. Sayed et.al, International Journal of Enhanced Research in Science Technology & Engineering **3**(1), 266 (2014).
- [2] X. S. Yao, L. Maleki, J. Opt. Soc. Am. B **13**(8), 1725 (1996).
- [3] W. Liang, D. Eliyahu, A. B. Matsko, V. S. Ilchenko, D. Seidel, L. Maleki, Laser Resonators, Microresonators, and Beam Control XVI, Proc. SPIE 8960 896010 (2014).
- [4] P. H. Merrer, A. Bouchier, H. Brahim, O. Llopis, G. Cibiel, Proc. of the 2009 IEEE EFTF-IFCS, 866 (2009).
- [5] A. Bouchier, K. Saleh, P. H. Merrer, O. Llopis, G. Cibiel, Proc. of the 2010 IEEE-IFCS, 544 (2010).
- [6] X. S. Yao, L. Maleki, IEEE J. of Quant. Electron. **36**, 79 (2000).
- [7] Qin Wang, Chuanchuan Yang, Optics Letters **38**(24), 15 (2013).
- [8] Mohamed Mahmoud, Ashraf Mahmoud, Lutong Cai, Msi Khan, Tamal Mukherjee, James Bain, Gianluca Piazza, Opt. Express **26**, 25060 (2018).
- [9] Alexander A. Krylov, Dmitry S. Chernykh, Elena D. Obratsova, Opt. Lett. **42**, 2439 (2017).
- [10] J. W. Fisher, L. Zhang, A. Poddar, U. Rohde, A. S. Daryoush, 2014 IEEE Benjamin Franklin Symposium on Microwave and Antenna Sub-systems for Radar, Telecommunications, and Biomedical Applications (BenMAS), Philadelphia, PA, 1 (2014).
- [11] Zhiqiang Fan, Qi Qiu, Jun Su, Tianhang Zhang, Yue Lin, Opt. Lett. **44**, 1992 (2019).

*Corresponding author: myshalaby@imamu.edu.sa